Chemical Deposition of Multilayer HgS Films

M.A. Sozanskyi*, K.M. Siryk, P.Yo. Shapoval, R.R. Huminilovych, V.E. Stadnik, M.M. Laruk

Lviv Polytechnic National University, 12, S. Bandera Str., 79013 Lviv, Ukraine

The 1-5-layer mercury sulfide (HgS) films were obtained on glass substrates by a chemical bath deposition method. The aqueous solutions of mercury (II) nitrate, thiourea and trisodium citrate were used to prepare working solutions. The theoretical boundary conditions of forming water-insoluble mercury sulfide and mercury oxide in the mercury-thiourea-citrate system were considered. The phase composition, surface morphology and optical properties of the 1-5-layer HgS films were investigated. According to the X-ray analysis, the film samples of deposited 1-5 layers were single phase and consisted of the HgS compound in trigonal (cinnabar) modification. The crystallite sizes of the 1-5-layer HgS films were calculated, and they are in the range of 11.0-33.3 nm, respectively. The films surface was solid and homogeneous and had a small amount of fine precipitate particles, which increased somewhat with each newly deposited HgS layer. The optical transmission spectra of obtained multilayer films were measured in the wavelength area from 340 to 900 nm. The HgS films transmission rises with the increase of wavelength with bends or sharper rises in the region of 350-500 nm, which is typical for films of semiconductor compounds. In addition, the spectral curves shift downward with an increase in the number of layers as the multilayer HgS film samples transmit less light with each newly deposited HgS layer. The optical bandgap values of the 1-5-layer HgS films were determined. The bandgap decreases from 2.86 eV (1-layer HgS film) to 1.78 eV (5-layer HgS film).

Keywords: Mercury sulfide, Semiconductor films, Chemical deposition, Optical properties, XRD.

DOI: 10.21272/jnep.15(6).06010

PACS numbers: 81.15.Lm, 78.66.Hf, 68.55.ag, 61.05.cp

1. INTRODUCTION

A significant part of modern research is focused on the nanoscale form of inorganic materials (nanoparticles or films). Some of the simple ways to obtain them are electrodeposition [1, 2], galvanic replacement [3, 4], chemical deposition [5, 6], etc. Mercury sulfide (HgS) belongs to the A2B6 semiconductor compounds (chalcogenides of the zinc subgroup). Nanomaterials, based on HgS are the least studied among the A2B6. One of the reasons is that it is more difficult to obtain mercury chalcogenides in nanoscale form than zinc and cadmium chalcogenides. Another reason may be the toxicity of mercury. However, authors [7, 8] have performed toxicity comparisons of HgS with mercury chloride ($HgCl_2$) and methylmercury (MeHg) and found that acute and chronic toxicity of HgS is substantially less than environmental soluble mercury compounds. This is explained by the fact that HgS is a highly water-insoluble compound and is difficult to be absorbed by the human body. Thus, only HgS of mercury compounds can be used in oral medication at appropriate small therapeutic doses or additives [8]. In particular, there are appropriate investigations of HgS protective effects against Parkinson's disease [9]. On the other hand, there are studies on the possibility of using nano-HgS in carbon-based composites as a high-performance supercapacitive electrode [10] or when combining deposition of silver [11] or gold [12] in the nanoscale form and HgS, such materials as the colorimetric nanoprism detector [13] or merged PiN Schottky (MPS) type diode [14] can be obtained, respectively.

In this work, we studied the patterns of X-ray diffraction (XRD), spectral dependences of optical transmission and microphotographs of scanning electron microscopy (SEM) of multilayer HgS films, where each layer of the HgS films was obtained under the optimal conditions determined by us earlier [15].

2. EXPERIMENTAL DETAILS

2.1 Materials

To obtain the HgS films, we used the following chemical reagents: mercury (II) nitrate ($Hg(NO_3)_2$), trisodium citrate ($Na_3C_6H_5O_7$), and thiourea ($(NH_2)_2CS$). Glass plates were used as the substrate material with unit dimensions of 18 mm × 18 mm.

2.2 Methods

The chemical bath deposition (CBD) method was used to obtain the HgS films. The conditions for HgS film deposition are given in Table 1. The necessary amounts of chemicals were dissolved in distilled water to obtain working solutions. Then, the required volume of working solution was poured into the bath and heated for a specified process duration at a given temperature. After the end of the deposition process, the substrates were removed from the bath and then cleaned with distilled water and dried in air. To deposit the next film layer, the substrates with the obtained HgS films were immersed into a new, freshly prepared solution, and the CBD was carried out at the same conditions (Table 1).

---

* martyn.a.sozanskyi@lpnu.ua

X-ray diffraction patterns (XRD, diffractograms) of the deposited HgS multilayer films were obtained using an Aeris Research X-ray diffractometer (Cu$K\alpha$-radiation) in the 2θ angle range from 0 to 90 degrees with a step of 0.01 degree. The processing of experimental diffractograms in order to identify the phase and refine its lattice parameters was carried out by the Rietveld calculation method using the FullProf program from the WinPLOTR interface [16].

Table 1 – The conditions for the HgS film deposition

Index	Value
$C(Hg(NO_3)_2)$, mol/L	0.01
$C((NH_2)_2CS)$, mol/L	0.02
$C(Na_3C_6H_5O_7)$, mol/L	0.015
Volume of working solution, mL	50
Process duration, min	5
pH of working solution	7.1
Temperature, °C	90

The optical transmission spectra $T(\lambda)$ of the HgS films were measured in the range of wavelengths (λ) 340-900 nm using a Xion 500 spectrophotometer. The accuracy of the T measurement was ±0.5 %. The Tauc relationship was applied to determine the optical bandgaps (E_g) of the deposited HgS films, as shown in [17].

The microphotographs of the surface morphology of the HgS films were taken on a REMMA-102-02 scanning electron microscope (SEM).

The pH value of the working solution was measured by a pH-150 MI pH meter equipped with a glass combined electrode.

3. RESULTS AND DISCUSSION

3.1 Boundary Conditions Consideration

Under the used conditions of HgS film deposition (Table 1), we have an aqueous system of mercury-thiourea-citrate. In this system, the formation of mercury water-soluble complexes with thiourea and citrate is possible, as well as mercury oxide (HgO) as an insoluble by-product of unstable mercury hydroxide. Earlier, when plotting one of the boundary zones of the $HgS_{1-x}Se_x$ phase in the mercury-thiourea-citrate system [18], we constructed boundary conditions of the HgS (as a partial case of $HgS_{1-x}Se_x$ formation) and HgO. They are shown in Fig. 1. There, the $C_{Hg^{2+}}^{min}$ value is the minimum Hg^{2+} salt concentration required for forming an insoluble phase. The grey zone is the formation area of HgS, and the red zone is the formation area of HgO. Insoluble HgS can be formed over the whole pH range. However, in practice, it is formed quickly in large quantities in an alkaline area. So, we decided to carry out HgS deposition at a neutral pH medium and concentration of mercury salt 10^{-2} mol/L. According to Fig. 1, the $C_{Hg^{2+}}^{min}$ value is around 10^{-14} mol/L in the neutral area. In practice, when Hg^{2+} salt concentration was lower below 10^{-2} mol/L, the HgS phase was formed, but less in the film form and more in the form of turbidity and precipitation [15].
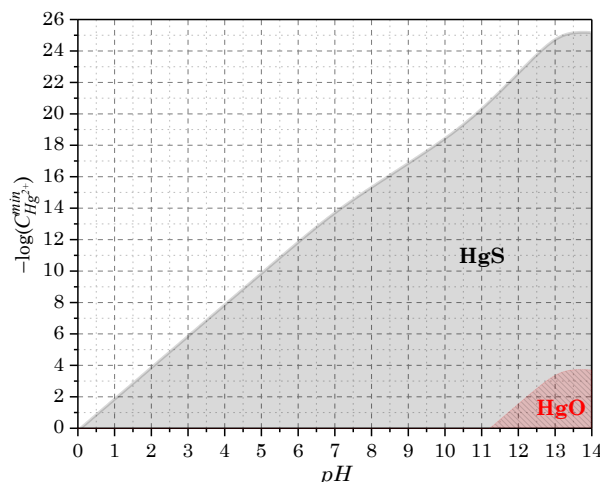

Fig. 1 – The boundary conditions of the HgS and HgO solid phases formation in the mercury-thiourea-citrate system

3.2 Structural and Morphological Properties

X-ray phase and structural analysis of deposited film samples was carried out. The experimental diffractograms of the 1-5-layer HgS films are shown in Fig. 2. Increasing the number of the HgS layers leads to sharper diffraction peaks. The sharpest diffraction peaks were observed at 5-layer HgS film, which is an indication of the formation of well-crystalline material. According to phase analysis, the trigonal (cinnabar) HgS phase (HgS structural type) was identified. The defined lattice cell parameters (a, c) of obtained layered HgS coatings are given in Table 2. They are close to the typical values for the HgS of the cinnabar form [3].

The average crystallite sizes (d) of the 1-5-layer HgS films were calculated using the Debye-Scherrer's formula [2, 17]:

$$d = \frac{k\lambda}{\beta \cos\theta}$$

where β is the full width at half maximum (FWHM) of the diffraction peak, k is the shape factor (equal to 0.9), λ is the wavelength of the Cu$K\alpha$- X-ray radiation source used in XRD ($\lambda = 0.15406$ nm), and θ is the angle of the diffraction peak. The results of the d calculation are shown in Table 2. According to them, we have an increase in the crystallite size of our film samples from 11.0 nm to 33.3 nm at the number of the HgS film layers from 1 to 5, respectively. This can be explained by the improvement in the crystal quality of each next layer, which corresponds to their sharper diffraction peaks.

Table 2 – Lattice parameters, the FWHM and average crystallite size values (d) of the 1-5-layer HgS films

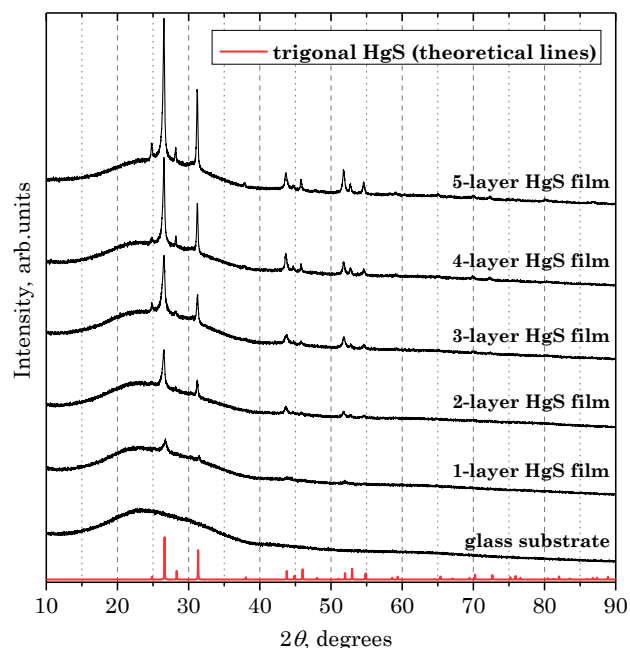| Number of film layers	2θ, deg	hkl	Lattice parameter		FWHM β, deg	FWHM β, rad	d, nm
			a, nm	c, nm			
1	26.46	101	0.41572(3)	0.94887(7)	0.7434	0.012975	11.0
2	26.56	101	0.41404(2)	0.94602(3)	0.4063	0.007091	20.1
3	26.55	101	0.41408(1)	0.94652(2)	0.3431	0.005988	23.8
4	26.53	101	0.41443(2)	0.94803(6)	0.2745	0.004791	29.7
5	26.52	101	0.41463(2)	0.94893(5)	0.2449	0.004274	33.3

Fig. 2 – XRD patterns of the 1-5-layer HgS films samples obtained on glass substrates and XRD pattern of the clean glass substrate for comparison

The microphotographs of surface morphology of the 1-, 3-, and 5-layer HgS films by scanning electron microscopy are shown in Fig. 3. As seen from micrographs, the film's surface was solid and homogeneous and had a small amount of fine precipitate particles of irregular shape, which increased somewhat with each newly deposited HgS layer. Also, an increase in the size of the film-forming grain can be seen on the general background of the microphotographs. This agrees with the results of X-ray structural studies.

3.3 Optical Properties

The optical transmission spectra $T(\lambda)$ of the 1-5-layer HgS films were measured (Fig. 4). The films transmission (T) increases in the investigated wavelength (λ) range from 340 to 900 nm. Spectral curves have sharper rises or bends at λ values from 350 to 500 nm. At longer wavelengths, transmission also increases, but not so sharply. With an increase in the number of the HgS film layers, the spectral curves shift downward. This can be explained by the fact that the multilayer HgS film sample transmits less light with each newly deposited HgS layer.

The optical bandgaps (E_g) of the 1-5-layer HgS films were determined (Fig. 5). The E_g values decreased from 2.86 eV (1-layer HgS film) to 1.78 eV (5-layer HgS film). Moreover, the E_g decrease is greater between the first deposited layers than between the last ones. Such a fairly wide change in E_g was observed earlier for the mercury chalcogenide films of HgS [15] and HgSe [19], deposited with different durations, i.e., a different amount of deposited coating over time. But for other films of A2B6 semiconductor compounds, for example, CdS, this change in E_g was in a much narrower range [20]. Thus, the following general effect is more pronounced in films o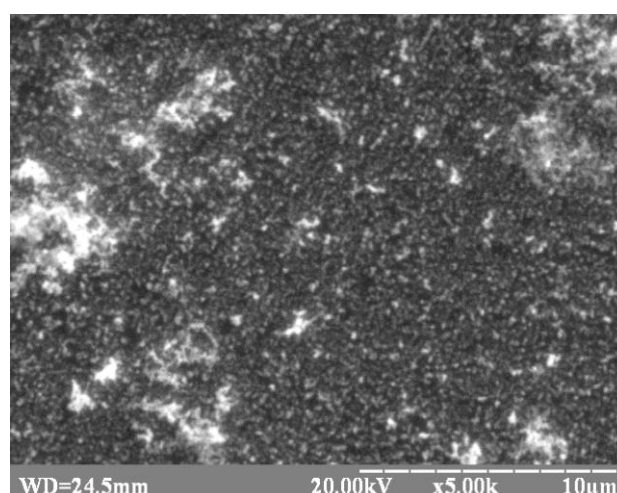f mercury chalcogenides: the smaller the size of the semiconductor nanocrystals and nanostructures, the larger the bandgap energy becomes [21].
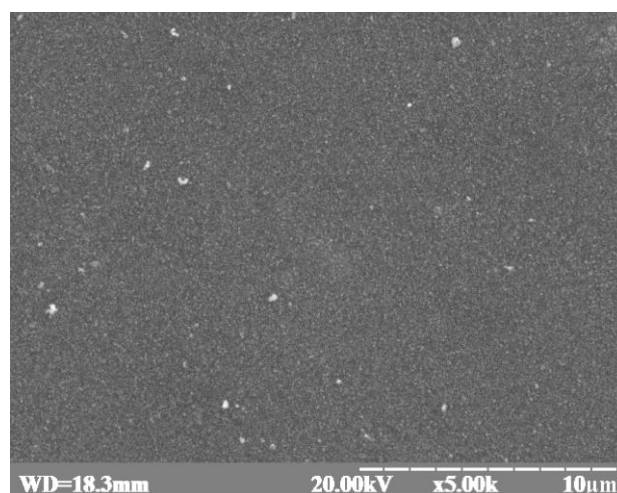
a
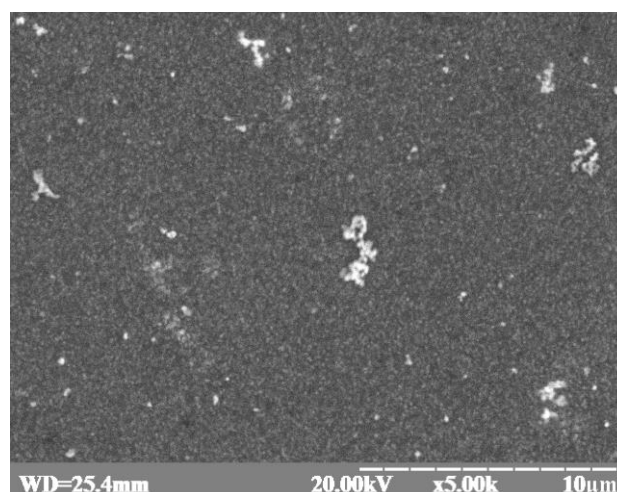
b

c

Fig. 3 – SEM images (x5000 magnification) of surface morphology of the HgS films (a – 1 layer, b – 3 layers, c – 5 layers)
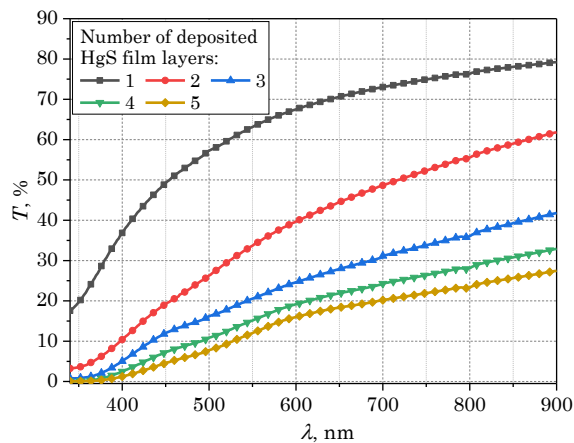
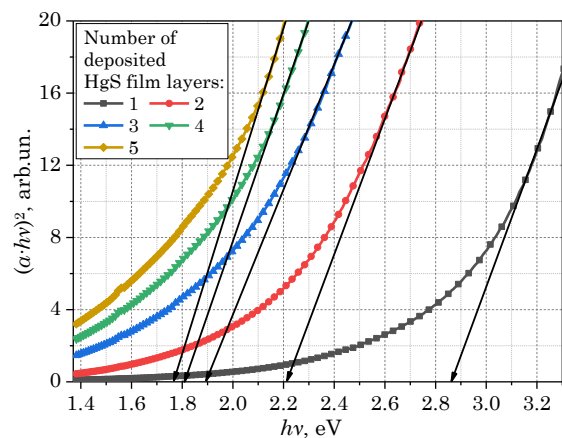**Fig. 4** – Optical transmission spectra of the 1-5-layer HgS films

Fig. 5 – $(ahv)^2 = f(hv)$ dependences and determination of the optical bandgap values of the 1-5-layer HgS films

4. CONCLUSIONS

The theoretical boundary conditions of forming water-insoluble compounds of mercury sulfide and mercury oxide in the mercury-thiourea-citrate system were considered.

The 1-5-layer HgS films were obtained on glass substrates by the chemical bath deposition method under defined earlier optimal synthesis conditions of one HgS layer. The obtained multilayer film samples were single-phase and contained the HgS (cinnabar) phase without any impurities. The sharp and strong XRD peaks indicate a good crystal quality of the material, which improved with each newly deposited HgS layer. Simultaneously, its crystallite size increased. The optical transmission spectra of the 1-5-layer HgS films were measured, and their optical bandgap values were determined, which varied within a sufficiently wide range from one to five layers of the HgS film. Accordingly, it has been established that this effect was more pronounced than the A_2B_6 chalcogenides of other metals.

Based on the studies carried out in this work, the deposited multilayer HgS films as A_2B_6 semiconductor material can be suitable for further research with a view to possible use in semiconductor elements for various electronic applications.

REFERENCES

1. S.S. Gavande, Y.H. Navale, A.S. Salunkhe, S. Gavande, P.S. Kulkarni, B.R. Karche, *J. Nano- Electron. Phys.* **12** No 2, 02011 (2020).
2. S.G. Pawar, C.V. Chanmal, S.S. Bandgar, R.N. Mulik, P.A. Desai, A.A. Admuthe, I.A. Dhole, *J. Nano- Electron. Phys.* **14** No 2, 02002 (2022).
3. M.V. Shepida, O.I. Kuntyi, S.A. Korniy, *J. Nano- Electron. Phys.* **14** No 1, 01021 (2022).
4. M. Shepida, O. Kuntyi, G. Zozulya, E. Kaniukov, *Appl. Nanosci.* **10**(8), 2563 (2020).
5. P. Shapoval, R. Guminilovych, I. Yatchyshyn, *Chem. Chem. Technol.* **7** No 3, 345 (2013).
6. P. Shapova, M. Sozanskyi, I. Yatchyshyn, B. Kulyk, M. Shpotyuk, R. Gladyshevskii, *Chem. Chem. Technol.* **10** No 3, 317 (2016).
7. J. Liu, L.-X. Wei, Q. Wang, Y.-F. Lu, F. Zhang, J.-Z. Shi, C. Li, M.G. Cherian, *J. Ethnopharmacol.* **210**, 340 (2018).
8. J. Liu, J.-Z. Shi, L.-M. Yu, R.A. Goyer, M.P. Waalkes, *Exp. Biol. Med.* **233** No 7, 810 (2008).
9. A.-L. Hu, S. Song, Y. Li, S.-F. Xu, F. Zhang, C. Li, J. Liu, *J. Ethnopharmacol.* **254**, 112674 (2020).
10. S.A. Pande, B. Pandit, B.R. Sankapal, *J. Colloid. Interf. Sci.* **514**, 740 (2018).
11. N. Adibah, B.E. Firdianti, S. Suprapto, *J. Nano- Electron. Phys.* **15** No 3, 03001 (2023).
12. M.V. Shepida, O.I. Kuntyi, O.Y. Dobrovets'ka, S.A. Kornii, Y.I. Eliyashevs'kyi, *Mater. Sci.* **55** No 3, 417 (2019).
13. S. Chen, J. Tang, Y. Kuang, L. Fu, F. Ma, Y. Yang, G. Chen, Y. Long, *Sensor. Actuat. B-Chem.* **221**, 1182 (2015).
14. Ö. Sevgili, İ. Taşçıoğlu, S. Boughdachi, Y. Azizian-Kalandaragh, Ş. Altındal, *Phys. B: Condens. Matter.* **566**, 125 (2019).
15. M. Sozanskyi, V. Stadnik, R. Guminilovych, P. Shapoval, M. Laruk, Yo. Yatchyshyn, *Visnyk of the Lviv University. Series Chemistry* **60** No 1, 146 (2019).
16. T. Roisnel, J. Rodríguez-Carvajal, *Mater. Sci. Forum* **378-381**, 118 (2001).
17. A.V. Raval, I.A. Shaikh, V.M. Jain, N.M. Shastri, P.B. Patel, L.K. Saini, D.V. Shah, *J. Nano- Electron. Phys.* **12** No 2, 02010 (2020).
18. M.A. Sozanskyi, P.Yo. Shapoval, V.E. Stadnik, O.P. Kyrulo, M.M. Laruk, *J. Nano- Electron. Phys.* **13** No 5, 05032 (2021).
19. M. Sozanskyi, V. Stadnik, R. Chaykivska, R. Guminilovych, P. Shapoval, I. Yatchyshyn, *Chem. Chem. Technol.* **11** No 4, 445 (2017).
20. M.A. Sozanskyi, P.Yo. Shapoval, R.R. Guminilovych, M.M. Laruk, Yo.Yo. Yatchychyn, *Voprosy Khimii i Khimicheskoi Tekhnologii* **2019** No 2, 39 (2019).
21. B.J. Abdullah, *Mat. Sci. Semicon. Proc.* **137**, 106214 (2022).

Хімічне осадження багатошарових плівок HgS

М.А. Созанський, К.М. Сірик, П.Й. Шаповал, Р.Р. Гумінілович, В.Є. Стаднік, М.М. Ларук

Національний університет «Львівська політехніка», вул. Степана Бандери, 12, 79013 Львів, Україна

1-5-шарові плівки сульфіду ртуті (HgS) отримано на скляних підкладках методом хімічного осадження. Для приготування робочих розчинів використовували водні розчини меркурій(II) нітрату, тіосечовини та тринатрій цитрату. Розглянуто теоретичні граничні умови утворення нерозчинних у воді сульфіду ртуті та оксиду ртуті в системі ртуть-тіосечовина-цитрат. Досліджено фазовий склад, морфологію поверхні та оптичні властивості 1-5-шарових плівок HgS. За даними рентгеноструктурного аналізу, зразки плівки осаджених 1-5 шарів були однофазними і складалися із сполуки HgS у тригональній (кіноварній) модифікації. Розраховано розміри кристалітів 1-5-шарових плівок HgS, які знаходяться в межах 11,0-33,3 нм відповідно. Поверхня плівок була суцільною і однорідною та мала невелику кількість дрібних частинок осаду, які дещо збільшувалися з кожним новим шаром HgS. Спектри оптичного пропускання отриманих багатошарових плівок виміряно в області довжин хвиль від 340 до 900 нм. Пропускання плівок HgS зростає зі збільшенням довжини хвилі з перегинами або більш різкими підйомами в області 350-500 нм, що характерно для плівок напівпровідникових сполук. Крім того, спектральні криві зміщуються вниз із збільшенням кількості шарів, оскільки зразки багатошарової плівки HgS пропускають менше світла з кожним новим шаром HgS. Визначено значення оптичної забороненої зони 1-5-шарових плівок HgS. Ширина забороненої зони зменшується від 2,86 еВ (1-шарова плівка HgS) до 1,78 еВ (5-шарова плівка HgS).

Ключові слова: Сульфід ртуті, Напівпровідникова плівка, Хімічне осадження, Оптичні властивості, XRD.